

PAPER • OPEN ACCESS

## Fabrication and characterization study of ZnTe/n-Si heterojunction solar cell application

To cite this article: BushraK H AlMaiyaly *et al* 2018 *J. Phys.: Conf. Ser.* **1003** 012084

View the [article online](#) for updates and enhancements.

### Related content

- [Effect of Aluminum on Characterization of ZnTe/n-Si Heterojunction Photo detector](#)  
Samir A Maki and Hanan K Hassun
- [Characterization of Copper Indium Diselenide Thin Films by Raman Scattering Spectroscopy for Solar Cell Applications](#)  
Satoshi Yamanaka, Makoto Konagai and Kiyoshi Takahashi
- [Crystal Structure, Optical, and Electrical Properties of SnSe and SnS Semiconductor Thin Films Prepared by Vacuum Evaporation Techniques for Solar Cell Applications](#)  
Ariswan, H Sutrisno and R Prasetyawati

# Fabrication and characterization study of ZnTe/n-Si heterojunction solar cell application

**BushraK H AlMaiyaly<sup>1</sup>, Bushra H Hussein Auday H Shaban**

Department of physics College of Education For Pure Science (Ibn AlHaitham)  
University of Baghdad Baghdad Iraq

drbushra2009 @yahoom

**Abstract.** Different thicknesses (150 250 and 350)  $\pm 20$  nm has been deposited on the glass substrate and nSi wafer to fabricate ZnTe/n-Si heterojunction solar cell by vacuum evaporation technique Structural optical electrical and photovoltaic properties are investigated for the samples. The structural characteristics studied via X ray analyses indicated that the films are polycrystalline besides having a cubic (zinc blende) structure also average diameter and surface roughness calculated from AFM images The optical measurements of the deposited films were performed in different thicknesses to determine the transmission spectrum as a function of incident wavelength in the range of wavelength (4001000) nm and the optical energy gap calculated from the optical absorption spectra was found to reduce with thickness The IV characteristic at (dark and illuminated) and CV measurement for ZnTe/n-Si heterojunction shows the good rectifying behaviour under dark condition. The measurements of opencircuit voltage ( $V_{OC}$ ) short-circuit current density ( $J_{SC}$ ) fill factor (FF) and quantum efficiencies of the ZnTe/n-Si heterojunction are calculated for all samples The results of these studies are presented and discussed in this paper

**Keywords** ZnTe/ n-Si heterojunction optical band gap structural properties solar cell

## 1 Introduction

Assembly IIIV compound semiconductors including cadmium selenide (CdSe) zinc selenide (ZnSe) zinc telluride (ZnTe) and cadmium telluride (CdTe) have established significant attention owing to their low cost however high absorption coefficients in their applications to a variety of solid state devices [1] Zinc telluride as a significant II–VI group semiconductor has a moderate and direct band gap of (17 to 24) eV at room temperature also has broadly used in modern technologies of optoelectronic [23] ZnTe thin films are broadly used in manufacturing different solid state optoelectronic devices (photo detectors solar cells light emitting diodes laser diodes microwave devices etc) due to its specific optical and electrical properties (high transparency in visible and infrared regions and low electrical resistivity etc) [45] ZnTe is an broadly investigated compound because of good optoelectronic properties mainly in the area of heterojunction solar cells The electrical and optical properties of ZnTe thin films can be optimized besides resistivity can be changed with dopant sort and concentration [67] Zinc telluride has a zincblende lattice and expansion of  $83 \times 10^6$  K Most heterostructures including ZnTe are characterized by very low lattice mis match For example it is 07% for InAsZnTe structure 009% for GaSbZnTe and 026% for GaAsZnTe [8] ZnTe thin films have been prepared by different techniques including magnetron sputtering [9] pulsed laser



deposition (PLD) thermal evaporation molecular beam epitaxy (MBE) [10] electron beam [11] closed space sublimation (CSS) [12] electrodeposition [13] etc. The aim of this study was focused on the construction and characterization of ZnTe/n-Si heterojunction for solar cells with different thin film thickness utilizing thermal evaporation technique.

## 2 Experimental

In this study n type Si wafer substrates with crystal orientation (111) indirect energy gap of 11eV diameter 762mm and thickness  $(508 \pm 15) \mu\text{m}$  which used to study the ZnTe/n-Si heterojunction these substrates were put in diluted 1% HF solution to eradicate the native oxide washed by deionized water several times then dry using soft paper. Secondly prepared glass slides were used as a substrate were used to study the structural electrical and optical properties of ZnTe films these glass slides were cleaned with chromic acid ultrasonic cleaner detergent water distilled water and then with acetone. High purity (99999)% ZnTe was used as a source material for the evaporation with thicknesses [150 250 and 350] nm were deposited by thermal vacuum evaporation using (Edwards – Unit 306) system. All thicknesses were determined with an optical interferometer method a suitable shape design for molybdenum boats were used for films evaporation also used spiral cord from Tungsten for deposition aluminum poles. X-ray diffraction (SHIMADZU Japan XRD 6000) diffractometer system with  $\text{CuK}\alpha$  radiation ( $\lambda = 15418 \text{ \AA}$ ) was used to identify the structural of the deposited films while topography surfaces investigations were carried out using atomic force microscopy (AFM). Optical transmission measurements and the band gap ( $E_g$ ) were performed with (UV-Visible 1800 spectrophotometer). Hall effect and the capacitance–voltage measurement of is determined by using HMS3000 Hall-measurement setting and by using (LRC meter Winsted 8105G) at a fixed frequency of (10 kHz). The IV characteristics of the ZnTe/n-Si heterojunction were measured using a DC power supply (F302 Farnell Instrument) and (Keithley digital electrometer 616). The measurements were performed in dark and under light.

## 3 Results and discussion

'Figure 1' displays the XRD spectrum of different thickness (150 250 and 350)  $\pm 20$  nm of ZnTe thin films. It is observed from XRD pattern of films that the all thickness films have polycrystalline and have cubic structure four noticeable peaks (111) (200) (220) and (311) and the prominent peak was (111) this is agreement with other studies [14,15]. The FWHM of the prominent peak decreases with increasing thickness due to a drop in the defects as a result of shrinking of the grain boundaries. Large crystallite size has been observed for film of thickness 350nm because of fast growth of crystallite and by reason of the reduction in grain boundaries this process results removal of the defects in the films. A similar behavior was observed in other studies for different thickness [16].

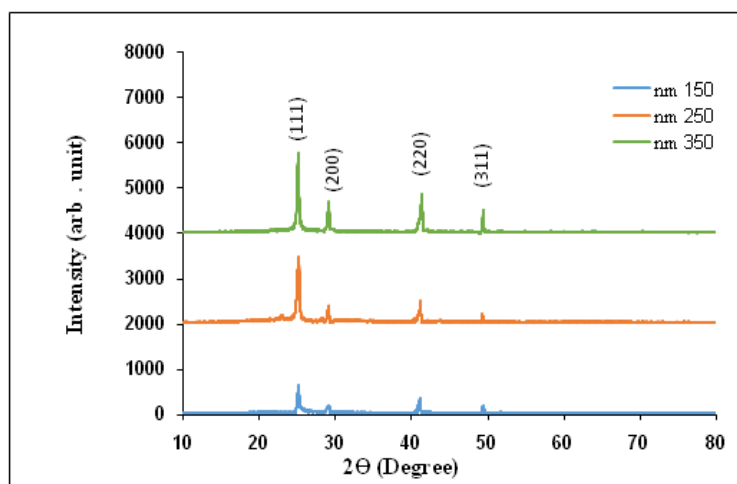


**Figure 1** XRD designs of ZnTe thin films at different thickness (150 250 and 350) nm

From the Scherer's relation [17] the average crystallite size (**CS**) of ZnTe thin films was calculated

$$(\mathbf{CS}) = \frac{094\lambda}{\beta\cos\theta} \dots\dots\dots(1)$$

Where  $\lambda$  is wavelength of radiation  $\beta$  is full width half maxima of the main peak and  $\theta$  the diffraction angle Table 1 shows the values of  $2\theta$   $d_{hkl}$  full width half maxima and the average crystallite size of the main peak

Table 1 The X ray diffraction parameters of ZnTe thin films of different thickness

film thicknesses (nm)	2 $\theta$ (deg)	$d_{hkl}$ (Å)	$\beta$ (deg)	<b>CS</b> (nm)
150	252991	35175	04093	2078
250	252747	35209	04240	2492
350	252325	35266	02439	3487

'Figure 2' shows the three dimensional (3D) AFM images of ZnTe thin films with different thickness we can be observed that the films are found to be uniform and densely packed without any cracks or pinholes and the average grain size was increased as the film thickness increase and the surface roughness values equal to (9393 11057 and 1374 nm) for the different thickness (150 250 and 350) nm respectively due to growth of some crystal planes the results agreement with X ray diffraction data Table 2 shows the values of grain sizes and surface roughness for different thickness

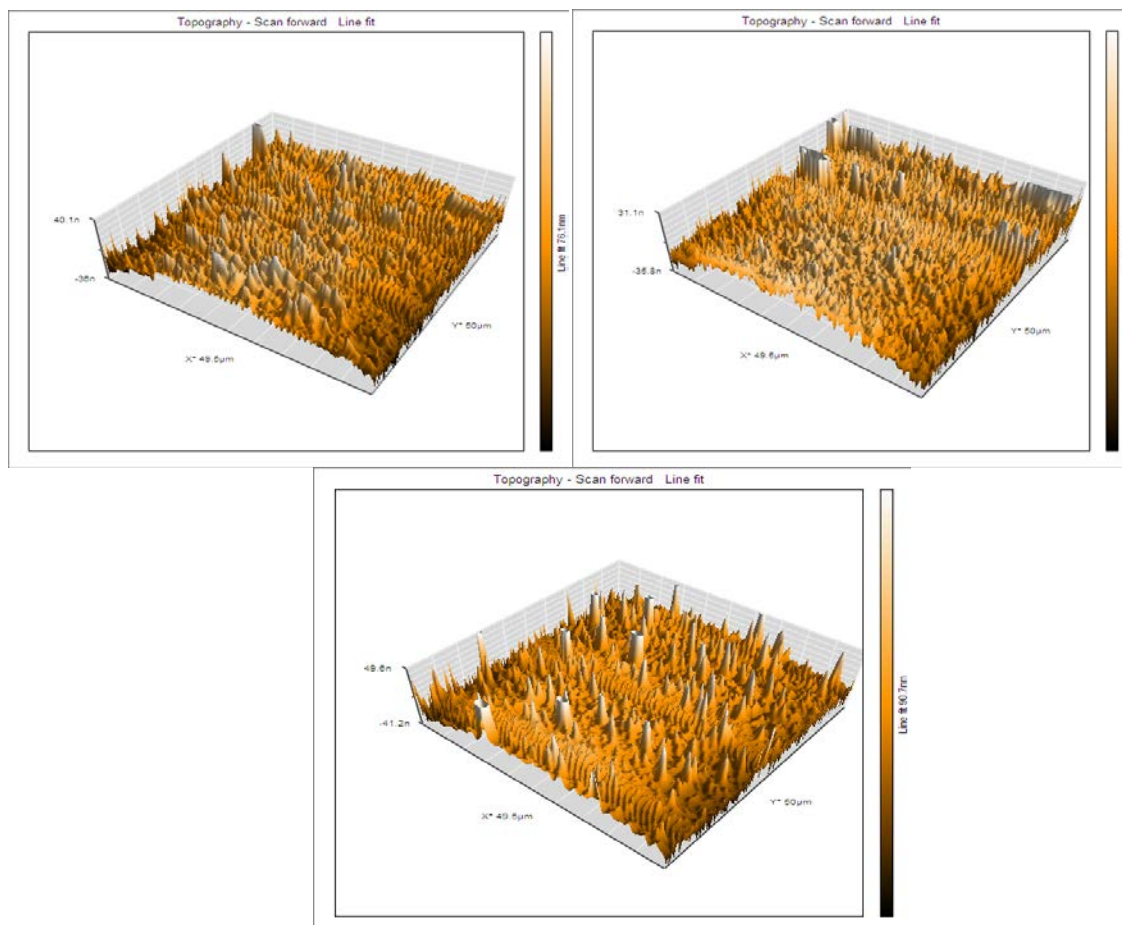


**Figure 2** 3D images of ZnTe thin films different thickness (150 250 and 350) nm

**Table 2** The average grain size and roughness of ZnTe thin films of 3 different thickness

Film thicknesses (nm)	Grain Size (nm)	Roughness average (nm)
150	688	9393
250	8165	11057
350	1294	1374

'Figure 3(ab)' demonstrates that the characteristic measured spectral transmittance and reflectance spectra of ZnTe films of three different thicknesses. It is shown that the maximum value of 6862% being reached for ZnTe thin films with lower thicknesses (150 nm) and the transmission decreasingly increasing the thicknesses (from 150 to 350) nm as a result of increase in the density of the film and due to highly transparent similar behavior has reported by other studies [18]. Figure 3(b) shows the reflectance spectra of films increased rapidly in visible region and then decreases with the increase of wave length from the range of (830 to 1000) nm with the increase in thicknesses.

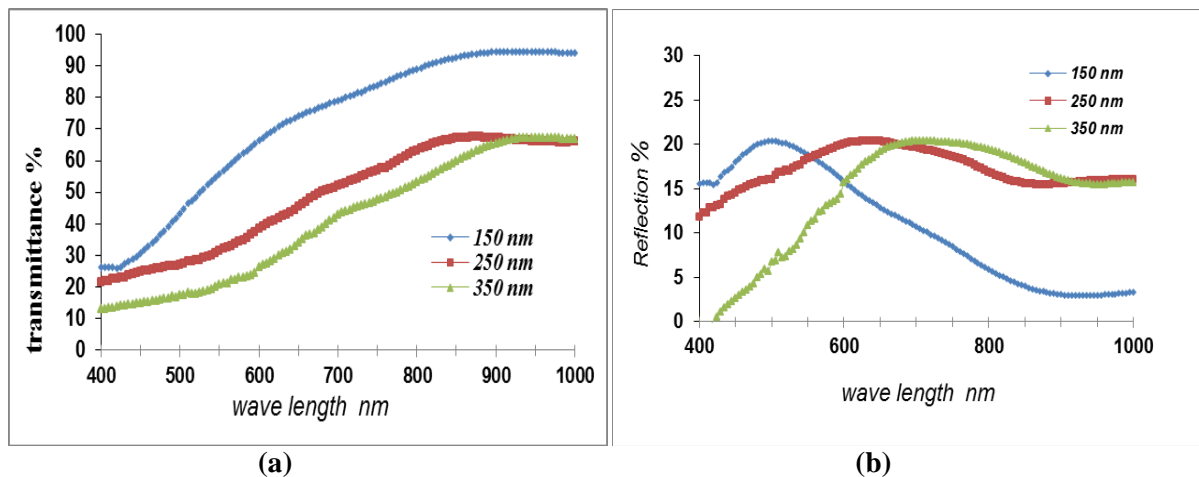


**Figure 3** The spectral transmittance and reflectance spectra of ZnTe thin films different thickness (150 250 and 350) nm

The optical band gap of the ZnTe thin films is calculated using the expression [19]

$$\alpha h\nu = B( h\nu - E_g )^r \dots\dots\dots(2)$$

Where **B** is constant **α** is the absorption coefficient **hν** is the photon energy **E<sub>g</sub>** is the optical band gap and **r** is constant may take values 2 3 1/2 3/2 depending on the material and the type of the optical transition. The optical band gap energy **E<sub>g</sub>** was obtained from the intercept on the photon energy axis after extrapolating of the straight line section of the curve of  $(\alpha h\nu)^2$  versus  $(h\nu)$  plot. Figure 4 expressions  $(\alpha h\nu)^2$  against the photon energy  $(h\nu)$  for different thicknesses (from 150 to 350) nm the energy band gap decrease from [202 eV to 182 eV] by means of high film thicknesses there are several energy levels resulted in several overlapping energy bands in the band gap of these films. The overlapping energy bands tend to decrease the energy band gap resulting in lower band gaps for increase on film thicknesses [20].

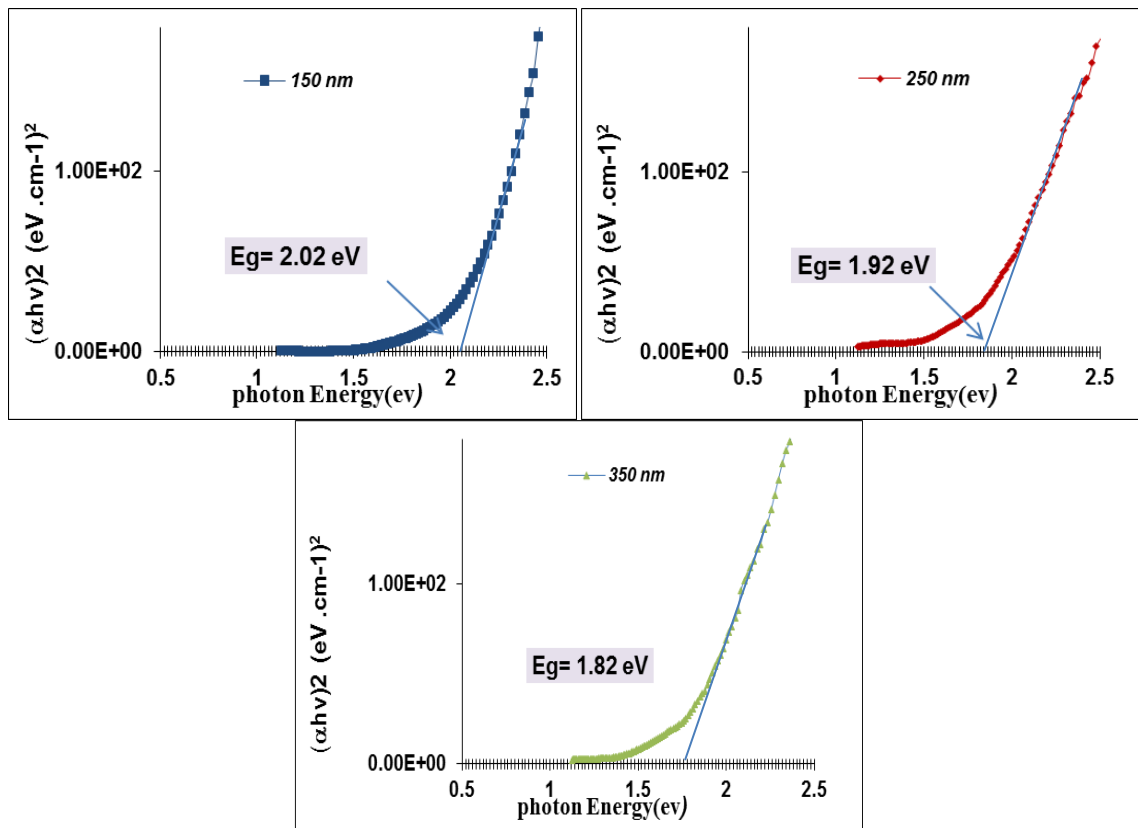


**Figure 4** Variation of  $(\alpha h\nu)^2$  verse photon energy ZnTe thin films different thickness

From Hall measurements can be estimated the type of charge carriers concentration and Hall mobility the positive sign of the hall coefficient indicates the conductive nature of the film is ptype Figure 5(ab) shows the variations of carriers concentration and Hall mobility with thickness respectively we can notice from the figure that the carrier concentration increased with increasing thickness due to drop in the resistivity the ultimate change in resistivity is due to the corresponding grain size Also we see increases in the Hall mobility with increasing thickness where there is a direct proportion between the carrier's concentration and the conductivity [21]

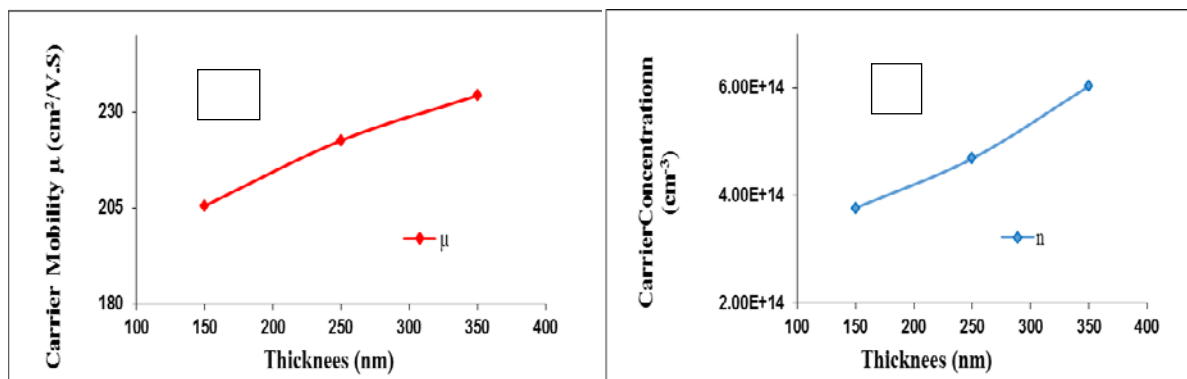


**Figure 5** The variations of **a** carriers concentration **b** Hall mobility with different thickness

Figure 6 shows change heterojunction capacity of unit area with reverse bias voltage at frequency (10 KHz) for different thickness the junction capacitance per unit area can be calculated using the expression [22]

$$C = \left[ \frac{q \epsilon_n \epsilon_p N_n N_p}{2(\epsilon_n N_n + \epsilon_p N_p)} \right]^{1/2} (V_{bi} - V)^{-1/2} \dots\dots\dots(3)$$

Where  $N_n$  and  $N_p$  are the donor and acceptor concentrations  $\epsilon_n$  and  $\epsilon_p$  are the dielectric constants of n and p type semiconductors respectively  $V_{bi}$  is the built-in junction potential and  $V_d$  is the applied voltage and the width of the depletion region can be calculated via [23]

$$W = \frac{\epsilon_s}{C_0} \dots\dots\dots(4)$$

$$\epsilon_s = \frac{\epsilon_n \epsilon_p}{\epsilon_n + \epsilon_p} \dots\dots\dots(5)$$

Where  $C_0$  is the capacitance on zero biasing voltage also  $\epsilon_s$  is dielectric constant of heterojunction for different thickness The scheme of  $1/C^2$  vs  $V$  is a straight line which means that the junction was of an abrupt type the intercept with the voltage axis gives the value of the built-in potential Table 3 shows the capacitance ( $C_0$ ) at (zero bias voltage) decreases with the increasing of ZnTe thickness due to the increasing of the depletion region where the increasing in the carrier concentration leads to a decrease of the capacitance The results have a good agreement with other studies [24]

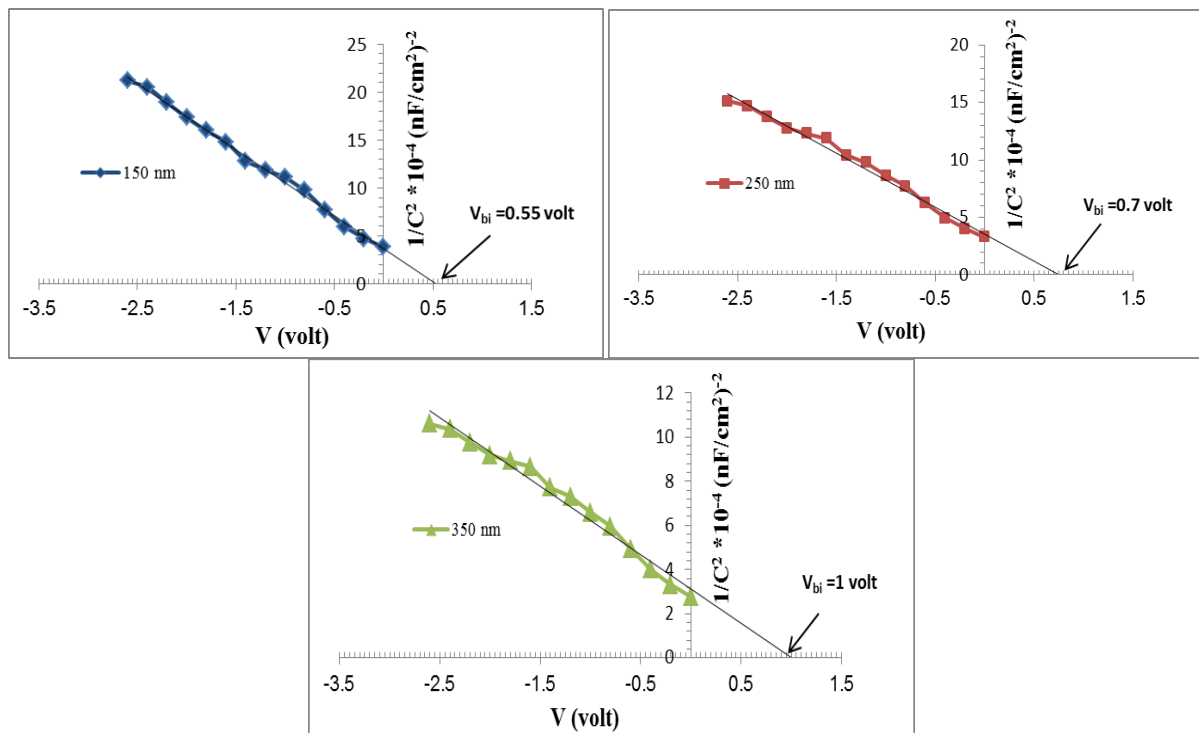


**Figure 6** Variation of  $1/C^2$  with reverse bias voltage for ZnTe /n-Si heterojunction with different thickness

**Table 3** Values of  $C_o$  W  $N_A$  and  $V_{bi}$  for ZnTe nSi heterojunction for different thickness

Thickness(nm)	$C_o(\text{nfc}\text{m}^2)$	W(nm)	$V_{bi}(\text{Volt})$	$N_A (\text{cm}^3)$
150	5668	86	055	144E+13
250	5308	9182	07	283E+13
350	522	9322	1	356E+13

The (I–V) characterizes of ZnTe/ n-Si heterojunction solar cell with different thickness (150 250 and 350)nm can be calculated by the two expressions [25]

$$I = I_s \left( \exp\left(\frac{qV}{\beta K_B T}\right) - 1 \right) - I_L \dots\dots\dots(6)$$

$$\beta = \frac{q}{K_B T} \frac{dV}{d(\ln I)} \dots\dots\dots(7)$$

Where  $I_s$  Saturation current  $I_L$  Illumination current  $I$  The total Solar cell current  $V$  applied voltage  $\beta$  is the ideality factor  $T$  Temperature in Kelvin  $K_B$  Boltzmann constant and  $q$  electron charge Figure 7 and Table 4 shows the barrier height ( $\Phi_{ba}$ ) and the reverse saturation current density it is clear that the ideality factor barrier height decrease and saturation current upsurge with increasing of thickness where this behavior attributed to improvement of crystal structure this result agrees with [26]. Also Figure 8 shows the (I–V) curve in dark and under illumination where the photocurrent produced by the (100 mWcm<sup>2</sup>) white lamp the current values rise exponentially by way of increasing in the forward bias voltage besides the device has high forward current Moreover the photovoltaic conversion efficiency ( $\eta$  %)and fill factor ( $FF$ ) can be calculated from two expressions [25]

$$\eta = \frac{P_m}{P_{in}} \times 100\% = \frac{I_m V_m}{P_{in}} \times 100\% \dots\dots\dots(8)$$

$$F.F = \frac{J_m V_m}{J_{sc} V_{oc}} \dots\dots\dots(9)$$

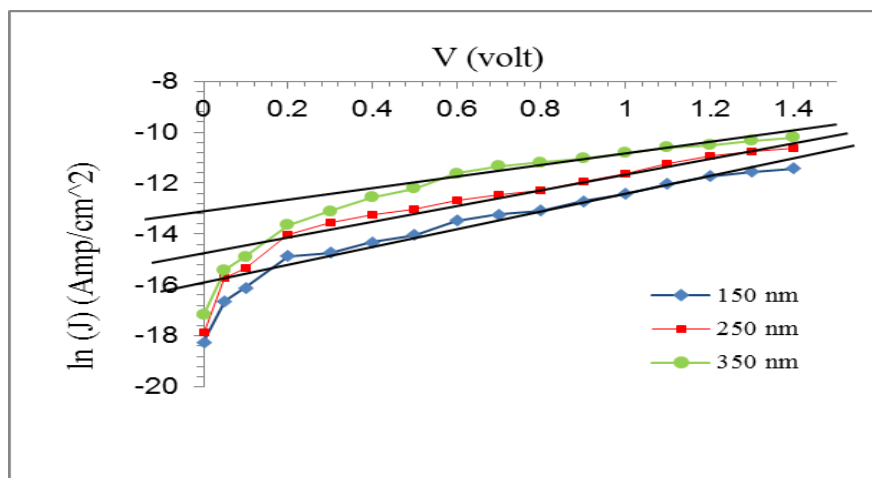


**Figure 7**  $\ln(J_s)$  with  $V$  for dark forward bias at different thicknesses



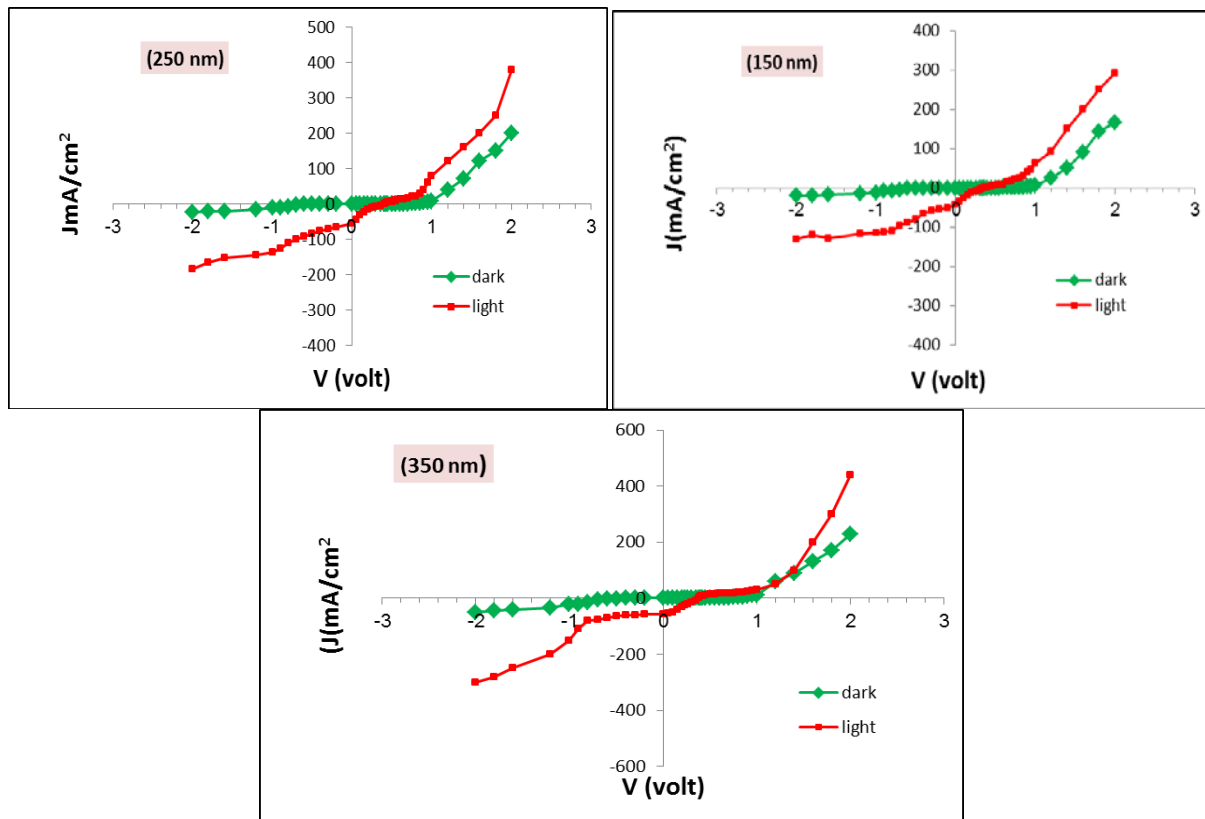


**Figure 8** IV characteristics of ZnTe nSi heterojunction solar cell dark and under illumination

**Table 4** Ideality factor Barrier height and Saturation current density values at different thickness

Thickness(nm)	Ideality Factor	Saturation Current Density( $J_s$ ) ( $\mu\text{Acm}^2$ )	Barrier Height ( $\Phi_b$ ) (eV)
150	1821	0112	0833
250	1698	031	0807
350	1532	137	0769

The open circuit voltage ( $V_{oc}$ ) short circuit current ( $I_{sc}$ ) fill factor (FF) and conversion efficiency ( $\eta_s\%$ ) results are shown in Table 5 we can find with increasing thickness the photovoltaic effect increasing that is clear in thickness (350 nm) where the conversion efficiency for ZnTe nSi heterojunction solar cell with (350nm) is much higher than (150) nm ZnTeSi heterojunction this behavior attributed to increase in photo generated current ( $I_{ph}$ ) our results nearly agreement with other studies [27]

**Table 5** The measurement with different thickness for ZnTe nSi heterojunction solar cell

Thickness (nm)	$V_{oc}$ (Volt)	$J_{sc}$ ( $\text{mAcm}^2$ )	$V_{max}$ (Volt)	$J_{max}$ ( $\text{mAcm}^2$ )	FF	$\eta$ %
150	04	18	02	123	0341667	246
250	022	40	015	25	0426136	375
350	02	55	013	40	0472727	52

#### 4 Conclusions

ZnTe thin films were prepared using thermal evaporation technique for different thickness (150 250 and 350)nm all films deposited on glass and silicon substrates at room temperature From XRD analysis it was found that the film is polycrystalline having the zinc blende structure with prominent peak was observed along (111) plane the ZnTe thin film for (350 nm) show large crystallite size with optimum surface roughness and low transmittance spectrum with appropriate band gap also the high Hall mobility value carriers concentration and low capacitance for (350 nm) thickness A photovoltaic device consisting of a ZnTe nSi heterojunction solar cell for (350 nm) have ideal behavior in ideality factor saturation current density and higher efficiency measurements this maximum was found to be 52% at ZnTe optimum thickness (350 nm)

#### References

- [1] Dong Hun Shin Jung Su Moon Park 2003 Electrochemical Preparation of Zinc Telluride Films on Gold Electrodes *Journal of the Electrochemical Society***150** 5 342346
- [2] Lin Bao Shun Zhang Rui Lu Wei Sun Qun Ling Fang 2015 ptype ZnTeGa nanowires controlled doping and optoelectronic device application *RSCAdv***5** 13324
- [3] MS Hossain R Islam K A Khan 2010 Structural Elemental compositions and Optical properties of ZnTeV *thin films Chalcogenide Letters***7** 1 21 29
- [4] N Amin K Sopian M Konagai 2007 *Sol Energ Mat Sol* **C91** 1202
- [5] H YChao J HCheng J Y Lu YHChang C L Cheng YFChen 2010ChenGrowth and characterization of typeII ZnOZnTe coreshell nanowire arrays for solar cell applications *Super lattice Microst***47** 160
- [6] A KSAqili A Maqsood and Z Ali2001Optical and Xray studies of low resistive films by immersion in Cu solution *Appl SurfSci***180** 73 80
- [7] NB Chaure J PNair R Jayakrishan V Ganesan and R K Pandey1998Effect of CuDoping on the morphology of ZnTe films electrodeposited from nonaqueousbath*Thin Solid Films***324** 78
- [8] K Z Yahiya ET Salem M SMuhammad 2008 Optical Constants of Zinc Telluride Thin Films in the Visible and NearInfrared Regions*Eng&Tech***265**
- [9] D Zeng W Jie H Zhou YYang 2011Effect of sputtering power on the properties of Cd<sub>1-x</sub>Zn<sub>x</sub>Te films deposited by radio frequency magnetron sputteringOriginal*Thin Solid Films***519** 4158
- [10] O Toma SAntohe 2014 Optical and morphological investigations of thermal vacuum evaporated ZnTe thin films*Letters***11** 3 11 611 618
- [11] A M Salem T M Dahy Y A Elgendy 2008Thickness dependence of optical parameters for ZnTe thin films deposited by electron beam gun evaporation technique. *Physica B***403** 3027
- [12] O de Melo E M Larramendi JMDuart MH Velez J Stangl HSitter Structure and growth rate of ZnTe films grown by isothermal closed space sublimation*JCryst Growth*2007 **307** 253
- [13] V S John T Mahalingam J P Chu 2005Synthesis and characterization of copper doped zinc telluride thin films *Solid State Electron***49** 3
- [14] Gowrish K Rao Kasturi V Bangera G K Shivakumar 2010 Studies on the Photoconductivity of vacuum deposited ZnTe thin films *Materials Research Bulletin***45** 10 13571360
- [15] JW Orton BJ Goldsmith JA Chapman MA Powell 1982 The mechanism of photoconductivity in polycrystalline cadmium sulphide layers *Journal of Applied Physics* 531602
- [16] G K R Å 2010 Studies on the photoconductivity of vacuum deposited ZnTe thin films *Materials Research Bulletin***45** 10 1357 1360
- [17] M J Yousef 1987 *Solid state physics*

- [18] W S Wang I Bhat 1997 The properties of ZnTe layers heteroepitaxially grown on Si using atmospheric metalorganic chemical vapor deposition *Materials Chemistry and Physics* **5** 80
- [19] Zimmermann Horst 2010 Integrated Silicon Optoelectronics *Engineering Electronics & Electrical Engineering* Springer Series in Optical Sciences
- [20] N A Okereke I A Ezenwa and A J Ekpunobi 2011 Effect of thickness on the optical properties of Zinc Selenide thin films *Journal of NonOxide Glasses* **3** 3 105 111
- [21] A K S Aqili A Maqsood Z Ali 2001 *Applied Surface Science* **180** 1
- [22] H Lewerenz 2004 Development of copper indium disulfide into a solar material *Solar Energy Materials and Solar Cells* **83** 4 395 407
- [23] N K Kwok 2002 *Complete guide to Semiconductor Devices* 2nd Edition Wiley IEEE Press USA
- [24] H M Zeyada MM ElNahass 2010 Characterization of 2,2,3,3-dihydro-1,5-dimethyl-3-oxo-2-phenyl-1H-pyrazol-4-ylimino-2,4-nitrophenyl acetonitrile and ZnO nanocrystallite structure thin films for application in solar cells. *J Appl Phys* **49** 10 301
- [25] D A Neamen 2003 *semiconductors physics and Devices Basic Principles* Third edition copyright© McGraw Hill Companies
- [26] Hussein Kh Rasheed Ramiz Ah AlAnssar Iman KaJebur Nisreen Kh Abdalameer 2016 Surface Morphology and Photoluminescence Properties of a GaAs/Zn Solar Cells International *Journal of Scientific & Engineering Research* **7** 5
- [27] Bernabe Mari and Hanif Ullah 2016 Numerical study of the influence of ZnTe thickness on CdS/ZnTe solar cell performance *Eur Phys J Appl Phys* **74** 2